The Journal of Immunology

Induction of Th1-Biased T Follicular Helper (Tfh) Cells in Lymphoid Tissues during Chronic Simian Immunodeficiency Virus Infection Defines Functionally Distinct Germinal Center Tfh Cells

Vijayakumar Velu, Geetha Hanna Mylvaganam, Sailaja Gangadhara, Jung Joo Hong, Smita S. Iyer, Sanjeev Gumber, Chris C. Ibegbu, Francois Villinger and Rama Rao Amara

J Immunol 2016; 197:1832-1842; Prepublished online 1 August 2016;
doi: 10.4049/jimmunol.1600143
http://www.jimmunol.org/content/197/5/1832

The Journal of Immunology is published twice each month by
The American Association of Immunologists, Inc.,
9650 Rockville Pike, Bethesda, MD 20814-3994.

Print ISSN: 0022-1767 Online ISSN: 1550-6606.

Induction of Th1-Biased T Follicular Helper (Tfh) Cells in Lymphoid Tissues during Chronic Simian Immunodeficiency Virus Infection Defines Functionally Distinct Germinal Center Tfh Cells

Vijayakumar Velu,* Geetha Hanna Mylvaganam,* Sailaja Gangadhara,* Jung Joo Hong,*,† Smita S. Iyer,* Sanjeev Gumber,‡ Chris C. Ibegbu,*,§ Francois Villinger,*,‡,¶ and Rama Rao Amara*,§

Chronic HIV infection is associated with accumulation of germinal center (GC) T follicular helper (Tfh) cells in the lymphoid tissue. The GC Tfh cells can be heterogeneous based on the expression of chemokine receptors associated with T helper lineages, such as CXCR3 (Th1), CCR4 (Th2), and CCR6 (Th17). However, the heterogeneous nature of GC Tfh cells in the lymphoid tissue and its association with viral persistence and Ab production during chronic SIV/HIV infection are not known. To address this, we characterized the expression of CXCR3, CCR4, and CCR6 on GC Tfh cells in lymph nodes following SIVmac251 infection in rhesus macaques. In SIV-naive rhesus macaques, only a small fraction of GC Tfh cells expressed CXCR3, CCR4, and CCR6. However, during chronic SIV infection, the majority of GC Tfh cells expressed CXCR3, whereas the proportion of CCR4$^+$ cells did not change, and CCR6$^+$ cells decreased. CXCR3$^+$, but not CXCR3$^-$, GC Tfh cells produced IFN-γ (Th1 cytokine) and IL-21 (Tfh cytokine), whereas both subsets expressed CD40L following stimulation. Immunohistochemistry analysis demonstrated an accumulation of CD4$^+$IFN-γ$^+$ T cells within the hyperplastic follicles during chronic SIV infection. CXCR3$^+$ GC Tfh cells also expressed higher levels of ICOS, CCR5, and α4β7 and contained more copies of SIV DNA compared with CXCR3$^-$ GC Tfh cells. However, CXCR3$^+$ and CXCR3$^-$ GC Tfh cells delivered help to B cells in vitro for production of IgG. These data demonstrate that chronic SIV infection promotes expansion of Th1-biased GC Tfh cells, which are phenotypically and functionally distinct from conventional GC Tfh cells and contribute to hypergammaglobulinemia and viral reservoirs. ***The Journal of Immunology*****, 2016, 197: 1832–1842.**

Lymphoid organs are the primary compartments for the generation of an effective adaptive immune response. CD4 T cells play a central role in the generation of adaptive immunity by providing help to CD8 T cells and B cells (1). CD4 T cells contain multiple subpopulations, including Th1, Th2, Th17, T follicular helper (Tfh), Th9, Th22, Th-CTL, and regulatory T cells (1–4), based on the function they exert and the cytokines they produce. Each of these Th cell subsets is tightly regulated by specific transcription factors and cytokines (2). Among the various subsets of CD4$^+$ T cells, CD4 Tfh cells play a major role in providing B cell help for the generation of long-lived memory B cell responses. Tfh cells reside within the germinal centers (GCs) and are essential for the formation of GCs where memory B cells proliferate and undergo affinity maturation and Ig class switching (5–8). Interactions between Tfh cells and B cells are mediated by many cellular and soluble factors, such as IL-21, IL-10, IL-4, CD40L, and ICOS (1, 9). Phenotypically, Tfh cells are characterized by the expression of chemokine receptor CXCR5, transcription factor Bcl-6, ICOS, and a high-level expression of programmed death-1 (PD-1) (9).

Multiple studies, including our own, characterized the Tfh cells in the lymph nodes (LNs) during chronic HIV infection in humans (10–13) and SIV infection in rhesus macaques (RMs) (14–18). These studies used different combinations of markers to define Tfh cells. Despite these differences, general conclusions could be derived. These studies demonstrated a marked increase in Tfh cells despite a decline in total CD4 T cells, and this increase in Tfh cell frequency was shown to be associated with increased Ab production (11, 12, 14–16). These Tfh cells express the Tfh transcription factor Bcl-6 and Tfh cell markers CXCR5, PD-1, ICOS, and CD40L and secrete soluble factors, such as IL-4, IL-10, and IL-21 (9). IL-21 production, in particular, was reported to be markedly elevated in LN Tfh cells from HIV-infected patients

*Emory Vaccine Center, Yerkes National Primate Research Center, Emory University, Atlanta, GA 30329; †National Primate Research Center, Korea Research Institute of Bioscience and Biotechnology, Ochang, Korea 363-883; ‡Department of Pathology, Emory University School of Medicine, Atlanta, GA 30322; §Department of Microbiology and Immunology, Emory University School of Medicine, Atlanta, GA 30322; and ¶New Iberia Research Center, University of Louisiana at Lafayette, New Iberia, LA 70560

ORCIDs: 0000-0003-4238-1924 (V.V.); 0000-0001-8603-628X (S. Gangadhara); 0000-0002-9795-6513 (J.J.H.); 0000-0001-9048-2717 (S. Gumber); 0000-0002-6309-6797 (R.R.A.).

Received for publication January 27, 2016. Accepted for publication July 1, 2016.

This work was supported by National Institutes of Health Grants R01AI074471, R01AI071852, P01AI088575, U19Al109633, and RC2CA149086 (to R.R.A.); Yerkes National Primate Research Center Base Grant P51 RR00165; and by Emory Center for AIDS Research Grant P30 AI050409.

Address correspondence and reprint requests to Prof. Rama Rao Amara, Emory Vaccine Center, Yerkes National Primate Research Center, Emory University, Room 3024, 954 Gatewood Road, Atlanta, GA 30329. E-mail address: ramara@emory.edu

The online version of this article contains supplemental material.

Abbreviations used in this article: GC, germinal center; LN, lymph node; NIH, National Institutes of Health; PD-1, programmed death-1; RM, rhesus macaque; Tfh, T follicular helper; YNPRC, Yerkes National Primate Research Center.

www.jimmunol.org/cgi/doi/10.4049/jimmunol.1600143

(10, 11, 16, 19) and SIV-infected macaques (16, 20, 21). In addition, a significant fraction of GC Tfh cells are positive for viral RNA, demonstrating that they support active virus replication during chronic HIV and SIV infections (11, 14, 16, 19). The expansion of GC Tfh cells in HIV infection correlated with an increase in GC B cells and plasma cells and a decrease in memory B cells, leading to the hypergammaglobulinemia that is characteristic in these patients (10, 12, 22).

The origin of Tfh cells is still under active investigation. Tfh cells are considered to be of a separate lineage; however, studies showed that Tfh cells can be generated from Th1 (23), Th2 (24), or other CD4 T cell lineages, suggesting a significant flexibility in vivo (25, 26). Recent studies showed that $CXCR5^+$ CD4 T cells in the blood possess a resting memory phenotype because they do not express ICOS or CD69 (27). These circulating $CXCR5^+$ CD4 T cells express chemokine receptors associated with Th1 (CXCR3) (28, 29), Th2 (CCR4) (30), and Th17 (CCR6) (31) lineages. Some of these studies explored the ability of these Th1-, Th2-, and Th17-like memory Tfh cells to deliver help to B cells in vitro and showed that $CXCR3^-$ Tfh cells, but not $CXCR3^+$ Tfh cells, provide B cell help (29, 31). However, studies also showed the emergence of $CXCR3^+ICOS^+CXCR5^+$ cells (effector CD4 T cells) at day 7 after influenza vaccination (28). Interestingly, ICOS expression was seen on a large proportion of $CXCR3^+$ Tfh cells. $ICOS^+$, but not $ICOS^-$ $CXCR3^+CXCR5^+$ cells provided help to memory B cells in vitro and predicted increase in anti-HA Ab titers at day 28 after immunization (28). In HIV-infected individuals, the frequency of $CXCR3^-PD\text{-}1^+CXCR5^+$ cells in blood was associated with development of neutralizing Abs (29). These data indicate that the phenotypic characteristics and B cell helper potential of $CXCR5^+$ CD4 T cells in the blood may be specific to the vaccine/infectious agent and the phase (effector versus memory) of analysis. In the context of HIV infection, the data suggest that circulating $CXCR3^-PD\text{-}1^+CXCR5^+$ cells may promote the production of highly functional broadly neutralizing Abs (29).

However, little is known regarding the expression of chemokine receptors associated with non-Tfh cells, such as CXCR3, CCR4, and CCR6, on LN-resident GC Tfh cells during chronic SIV/HIV infection. Thus, in the current study, we investigated the expression of chemokine receptors CXCR3, CCR4, and CCR6 by GC Tfh cells in the LNs of SIV-naive and chronically SIV-infected RMs and determined the relationship between specific Tfh phenotype and B cell helper function. Our results demonstrated the existence of $CXCR3^+$ GC Tfh cells and a significant expansion of these cells during chronic SIV infection. These $CXCR3^+$ GC Tfh cells are functionally distinct from $CXCR3^-$ GC Tfh cells in terms of phenotype and cytokine production. Specifically, $CXCR3^+$ GC Tfh cells, but not $CXCR3^-$ GC Tfh cells, produced Tfh cytokine IL-21 and Th1 cytokine IFN-γ. In addition, unlike $CXCR3^-$ GC Tfh cells, $CXCR3^+$ GC Tfh cells expressed higher levels of CCR5 and α4β7 and contained a significantly greater number of copies of SIV DNA. These data demonstrated an unexpected expansion of $CXCR3^+$-biased GC Tfh cells during chronic SIV infection that are phenotypically and functionally distinct from conventional GC Tfh cells and contribute to hypergammaglobulinemia and viral reservoirs.

Materials and Methods

Ethics statement

All animal experiments were conducted at the Yerkes National Primate Research Center (YNPRC), which is accredited by the American Association of Accreditation of Laboratory Animal Care, International, following guidelines established by the Animal Welfare Act and the National Institutes of Health (NIH) for housing and care of laboratory animals. Blood and tissue collections were obtained under anesthesia. RMs were fed standard monkey chow (Jumbo Monkey Diet 5037; Purina Mills, St Louis, MO) supplemented with fresh fruit or vegetable daily. Consumption was monitored and adjustments were made as necessary depending on sex, age, and weight. SIV-infected RMs were singly caged but had visual, auditory, and olfactory contact with at least one social partner, permitting the expression of noncontact social behavior. The YNPRC enrichment plan uses several general categories of enrichment. Appropriate procedures were performed to ensure that potential distress, pain, discomfort, and/or injury were limited to that unavoidable in the conduct of the research plan. Ketamine (10 mg/kg) and/or telazol (4 mg/kg) were used for collection of blood and tissues, and analgesics were used when determined appropriate by veterinary medical staff.

Animals

Indian adult RMs obtained from the Yerkes breeding colony were cared for under the guidelines established by the Animal Welfare Act and the NIH *Guide for the Care and Use of Laboratory Animals* using protocols approved by the Emory University Institutional Animal Care and Use Committee. SIV-infected animals were infected with SIVmac251 intrarectally, as described previously (32). Some animals were positive for Mamu A*01 allele, and all animals were negative for Mamu B08 and Mamu B17. See Supplemental Table I for additional details.

Abs

Cells were stained with fluorochrome-conjugated Abs specific for CXCR5 (clone MU5UBEE; eBioscience), CD3 (clone SP-34-2; BD Biosciences), CXCR3 (clone IC6; BD Biosciences), CCR6 (clone 11A9), CCR4 (clone 1G1), ICOS (clone C398.4A; eBioscience), CD95 (clone DX2; BD Biosciences), PD-1 (clone EH12.1; BioLegend), CD8 (clone SK1; BD Biosciences), CD4 (clone OKT4; BioLegend), CCR5 (clone 3A9; BD Biosciences), α4β7 (Act1; NHP reagent resource), LIVE/DEAD Fixable Near-IR Dead Cell stain (Invitrogen), Ki-67 (clone B56; BD Biosciences), Bcl-6 (clone K112-91), IL-21 (clone 3A3-N2; BD Biosciences), CD4 (clone L200; BD Biosciences), Alexa Fluor 700–conjugated IFN-γ (clone B27; BD Biosciences), and FITC-conjugated CD40L (clone TRAP1; BD Biosciences).

Phenotyping

Approximately 1×10^6 mononuclear cells isolated from the LN were stained with LIVE/DEAD Fixable Near-IR Dead Cell stain at room temperature for 15 min in PBS to stain for dead cells. Cells were washed with FACS wash and stained on the surface using Abs specific to CD3, CD4, CD95, CXCR5, CXCR3, CD20, and PD-1 for 25 min at room temperature. Cells were fixed with 1× BD FACS Lysing Solution for 10 min at room temperature, permeabilized with 1× BD permeabilizing solution for 8 min at room temperature, and washed with FACS wash. Cells were stained intracellularly using Ab to Ki-67 and Bcl-6 in FACS wash for 30 min at room temperature, washed twice with FACS wash, acquired using an LSRFortessa with four lasers (405, 488, 532, 633 nm), and analyzed using FlowJo software (TreeStar, Ashland, OR). At least 50,000 events were acquired for each sample, as done previously (16). The live memory CD4 T cells ($CD3^+$, $CD4^+$, $CD95^+$) were analyzed for expression of other surface and intracellular markers described above.

Intracellular cytokine staining

Mononuclear cells from fresh or frozen LN samples were suspended in RPMI 1640 medium (Life Technologies) with 10% FBS (HyClone; Thermo Fisher Scientific), 100 IU/ml penicillin, and 100 μg/ml streptomycin (Lonza). Stimulations were conducted in the presence of anti-CD28 Ab and anti-CD49d Ab (1 μg/ml; BD Pharmingen). A total of 50,000 sorted cells was stimulated with 10 ng/ml PMA and 1 μg/ml ionomycin in the presence of Brefeldin A (5 μg/ml; Sigma) and GolgiStop (0.5 μl/ml; BD Pharmingen) after 2 h of stimulation for 4 h at 37˚C in the presence of 5% CO_2. Then cells were washed once with FACS wash (PBS containing 2% FBS and 0.05% sodium azide) and surface stained with anti-CD3, anti-CXCR5, anti–PD-1, anti-CXCR3, and anti-CD95 at room temperature for 20 min. Cells were fixed with Cytofix/Cytoperm for 20 min at 4˚C and washed with Perm/Wash Buffer (both from BD Pharmingen). Cells were then incubated for 30 min at 4˚C with Abs specific to IFN-γ, IL-21, CD40L, and CD4, washed once with Perm/Wash Buffer and once with FACS wash, and resuspended in PBS containing 1% formalin. Cells were acquired on an LSRFortessa with four lasers (405, 488, 532, 633 nm) and analyzed using FlowJo software (TreeStar). At least 50,000 events were acquired for each sample.

Immunofluorescence and quantitative image analysis

Immunofluorescence and quantitative image analysis were performed as previously described (14) using 4–5-μm paraffin tissue sections. The sections were deparaffinized and rehydrated through sequential ethanol washes. Heat-induced epitope retrieval was performed with DIVA Decloaker in a high-pressure cooker (Biocare Medical). Sections were then blocked with SNIPER reagent (Biocare Medical) for 15 min and in PBS/0.1% Triton-X 100/4% goat serum for 30 min at room temperature. After the blocking step, the sections were incubated with mouse anti-human IFN-γ (clone B27; BD Biosciences), rabbit anti-human IL-21 (polyclonal Ab), and rat anti-human CD3 (clone CD3-12; both from AbD Serotec) Abs diluted 1:50–1:100 in blocking buffer at 4°C overnight. These sections were incubated with secondary Abs conjugated with fluorescent dyes diluted 1:1000–1:2000 (Jackson ImmunoResearch) in blocking buffer for 30 min at room temperature. Finally, nuclei were stained with Hoechst 33342 (Invitrogen) for 10 min at room temperature and mounted using warmed glycerol gelatin (Sigma) containing 4 mg/ml *n*-propyl gallate (Fluka). Every step was followed by three washes with TBS automation buffer (Biocare Medical). For each LN tissue section stained with Abs (IL-21, IFN-γ, and CD3), images were collected with an Axio Imager Z1 microscope (Zeiss) using 20× objectives. Lymphoid follicle area in cortex was acquired as much as possible (5–52 follicles), based on CD3 and Hoechst staining. GC size and mean fluorescence intensities of cytokines were calculated using the AxioVs40 V4.8.1.0 program (Zeiss) and Image J1.43u (NIH).

Cell sorting

Approximately 100 × 10^6 mononuclear cells isolated from the LN were stained with LIVE/DEAD, anti-CD3, anti-CD4, anti-CD95, anti-CXCR5, anti-CXCR3, anti-CD20 and anti–PD-1 for 25 min at 4°C. The memory CD4 T cells (CD95$^+$) were further gated, using CXCR5, PD-1, and CXCR3 markers, divided into CXCR3$^+$CXCR5$^+$PD-1^{++} (CXCR3$^+$GC Tfh) and CXCR3$^-$CXCR5$^+$PD-1^{++} (CXCR3$^-$ GC Tfh) CD4$^+$ T cell populations, and sorted using a FACSAria II (BD). For all sorted subsets, the purity was >95%. Sorted cells were used for in vitro stimulation for cytokine production using PMA/ionomycin stimulations and for T and B cell coculture experiments.

Ab measurements

SIV-specific Ab responses were assessed in serum by envelope-specific ELISAs using commercially purchased SIVmac239 gp140 Ag (cat. no. IT-001-140P; Immune Technology, New York, NY). Briefly, ELISA plates (Costar; Corning Life Sciences, Lowell, MA) were coated with SIV gp140 (0.5 μg/ml) in 10 mM sodium bicarbonate buffer (pH 9.3) overnight at 4°C. Plates were washed and blocked for 1 h with PBS-Tween, 4% whey, and 5% dry milk. SIV-infected macaque serum samples were added to duplicate wells in serial 5-fold dilutions and incubated for 2 h at room temperature. Plates were then washed, and bound Ab was detected using peroxidase-conjugated anti-monkey IgG (Accurate Chemical and Scientific, Westbury, NY) and tetramethylbenzidine substrate (KPL, Gaithersburg, MD). Reactions were stopped with 100 μl of 1 M H_3PO_4 and read at 450 nm. Each plate included a standard curve generated using goat anti-monkey IgG and known concentrations of rhesus IgG (both from Accurate Chemical and Scientific) starting from 100 ng/ml. SIV-specific IgG1 Ab responses were assessed in serum in a similar manner, except for detection biotin labeled mouse monoclonal anti-rhesus IgG1 (7H11 Biotin; NHP Reagent Resource) followed with HRP Avidin (Vector Laboratories) was used. Each plate included a standard curve generated using mouse monoclonal anti-monkey IgG (8F1) for coating and known amounts of purified rhesus IgG1 (NHP Reagent Resource), starting from 10 μg/ml, for capture.

Total macaque IgG concentrations in culture supernatants were assessed by coating ELISA plates with goat anti-monkey IgG at 50 μl/well. Culture supernatants were used undiluted or diluted 1:2, and bound IgG was detected using peroxidase-conjugated anti-monkey IgG, as described above. For measuring total macaque IgG1 Ab responses, the culture supernatants were assessed by coating ELISA plates with 50 μl of mouse monoclonal anti-rhesus IgG1 (7H11; 2 μg/ml; NHP Reagent Resource) in PBS overnight. Diluted or 1:2 diluted culture supernatants were added after blocking. Bound IgG1 was detected using biotin-labeled mouse monoclonal anti-rhesus IgG (8F1 Biotin; NHP Reagent Resource), followed by HRP Avidin (Vector Laboratories). Standard curves were fitted, and sample concentrations were interpolated as μg/ng (Ab)/ml of serum/culture supernatant using SOFTmax 2.3 software (Molecular Devices, Sunnyvale, CA). The concentrations of anti-SIV gp140-specific IgG, IgG1, total macaque IgG, and IgG1 are relative to our standard curve, not absolute values.

Quantitation of SIV RNA and DNA

The SIV copy number in plasma was determined using quantitative real-time PCR, as described previously (33). For viral load determinations in LN, total DNA was extracted from ∼50,000 sorted CXCR3$^+$ and CXCR3$^-$ GC Tfh cell subsets, and data were normalized to albumin, as described previously (34). Sorting experiments were performed on cryopreserved LN samples. All PCRs were performed in duplicates with a limit of detection of 60 copies/reaction.

T and B cell cocultures

Coculture experiments were performed on frozen LN cells. A total of 5 × 10^4 sorted CD4 T cells was cultured with 5 × 10^4 sorted autologous total B cells (1:1 ratio) in the presence of staphylococcal enterotoxin B (0.5 μg/ml). Supernatants harvested on day 9 were analyzed for total monkey Igs for IgG and IgG1. For determining the proliferation of total B cells by flow cytometry, cells were harvested on day 5.

Statistical analyses

The Wilcoxon test was used for comparisons between two or more subsets from the same animal. The unpaired nonparametric Mann–Whitney *U* test was used for comparisons between SIV-uninfected and SIV-infected animals. The Spearman rank test was used for all correlations. Boolean analyses were performed using SPICE software (National Institute of Allergy and Infectious Diseases, NIH). When box-and-whisker plots are used, the box size represents the limits of the data for the second and third quartiles, with the median shown as a horizontal line. The GraphPad Prism statistical analysis program (GraphPad) was used to determine p values. The p values <0.05 were considered significant.

Results

GC Tfh cells show a distinct profile for coexpression of chemokine receptors compared with non-GC Tfh cells in SIV-naive RMs

Tfh cells are characterized by the combined expression of CXCR5, ICOS, and high levels of PD-1 in mice and humans (9). Similar to humans and mice, few studies defined Tfh cells in RMs based on CXCR5 (16, 18, 35, 36), a key chemokine receptor required for homing of cells to B cell follicles/GCs. In addition, it is important to characterize the expression of chemokine receptors that influence the migration and lineage relationship of CD4 T cells. To understand the relative distribution of CXCR5$^+$ and CXCR5$^-$ CD4 T cells in the LN of SIV-naive RMs, we characterized five populations of memory CD4 T cells (CD3$^+$, CD4$^+$, CD95$^+$) based on CXCR5 and PD-1 expression: CXCR5$^-$PD-1$^-$ (X5$^-$PD-1$^-$), CXCR5$^-$PD-1$^+$ (X5$^-$PD-1$^+$), CXCR5$^+$PD-1$^-$ (X5$^+$PD-1$^-$), CXCR5$^+$PD-1$^+$ (X5$^+$PD-1$^+$), and CXCR5$^+$PD-1^{++} (X5$^+$PD-1^{++}) (Fig. 1A). Among these five subsets, the CXCR5$^-$ subsets constituted ∼50–60% of the total cells, and the frequency of X5$^+$PD-1^{++} was the lowest (∼5%) (Fig. 1B). The relative distribution of these five subsets within the memory CD4 T cells was comparable to that reported for CD4 T cells in LNs of humans (10–12, 29, 37).

We then characterized these cells for coexpression of markers associated with Tfh cells, such as Bcl-6, ICOS, and CCR7. Similar to human LN cells (10–12), the macaque X5$^+$PD-1^{++} cells expressed the highest levels of GC Tfh cells markers Bcl-6 and ICOS and the lowest levels of CCR7, suggesting that the X5$^+$PD-1^{++} subset represents macaque GC Tfh cells (Fig. 1C); hence, we refer to this subset as GC Tfh cells hereafter. Bcl-6 expression was confined primarily to GC Tfh cells (Fig. 1C) (1, 2). In contrast to Bcl-6 expression, ICOS was expressed on CXCR5$^+$ and CXCR5$^-$ memory CD4 T cells, with particularly high levels on PD-1$^{+/++}$ cells. However, an opposite trend was observed for CCR7 expression, which was generally low on PD-1$^+$ memory CD4 T cells and was lowest on GC Tfh cells. Of note, the X5$^-$PD-1$^+$ subset expressed relatively higher levels of ICOS and lower levels of CCR7 compared with other non-GC Tfh cell subsets, suggesting the existence of a non-Tfh cell memory population with the

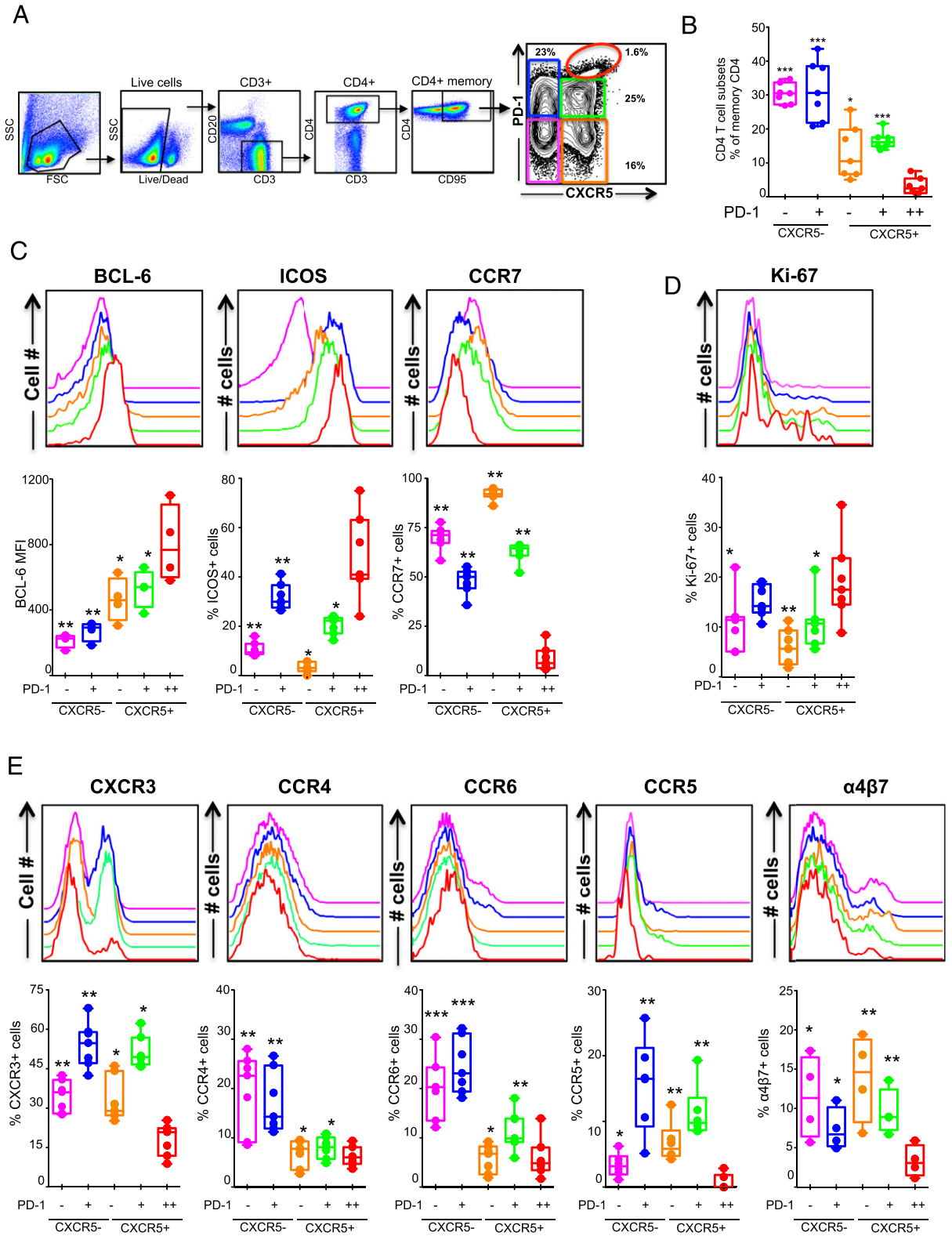

FIGURE 1. Characterization of five memory CD4 T cell subsets defined based on CXCR5 and PD-1 expression in the LN of SIV-naive RMs. (**A** and **B**) Relative distribution of five memory CD4 T cell subsets (CD95+ CD4+ cells) in the LN defined based on CXCR5 and PD-1 expression. Representative flow plot is shown in (A) and summary for a group ($n = 7$) of SIV-naive RM is shown in (B and **C**) Expression of Tfh cell markers Bcl-6 and ICOS, and non-Tfh cell marker CCR7 ($n = 7$). (**D**) Expression of proliferation marker Ki-67 ($n = 7$). (**E**) Expression of different chemokine receptors CXCR3, CCR4, CCR6, CCR5 and α4β7 ($n = 7$ except for α4β7 for which $n = 4$). p values shown are for $CXCR5^+$ $PD\text{-}1^{++}$ (GC Tfh) subset versus other subsets. The legend for histogram plots shown in (C)–(E) is shown in (B). $^*p < 0.05$, $^{**}p < 0.01$, $^{***}p < 0.001$.

potential to provide B cell help. We then investigated the ex vivo proliferation status of these five CD4 T cell subsets based on Ki-67 expression and found that ~10–20% of the $CXCR5^-$ and $CXCR5^+$ subsets in the LN expressed Ki-67, with the GC Tfh cells, were the most proliferative compared with any other subsets (Fig. 1D).

We next studied the expression of additional chemokine receptors (CXCR3, CCR4, and CCR6), because the expression of these receptors was shown to be associated with the Th1, Th2, and Th17 CD4 T cell helper lineage, respectively (30, 38), as well as CCR5 and the integrin α4β7 (Fig. 1E). A significant fraction of all non-GC Tfh cell memory subsets expressed CXCR3, and the expression was higher on PD-1$^+$ subsets than on PD-1$^-$ subsets; however, only a small fraction of GC Tfh cells expressed CXCR3. In contrast, CCR4 and CCR6 expression was restricted primarily to CXCR5$^-$ memory subsets. Similarly, the expression of CCR5 was primarily restricted to non-GC Tfh cells; within the non-GC Tfh cells, expression of CCR5 was higher on PD-1$^+$ cells compared with PD-1$^-$ cells. Only a small fraction of GC Tfh cells expressed CCR5, despite the fact that these cells are highly infected during chronic SIV infection (39). Similar to CCR5, α4β7 expression was restricted to non-GC Tfh cell subsets. Interestingly, the expression of α4β7 was relatively higher in PD-1$^-$ cells compared with PD-1$^+$ cells. Collectively, these results revealed that the GC Tfh CD4 subset was distinct from non-GC Tfh cells, with limited/low expression of CXCR3, CCR4, CCR6, CCR7, CCR5, and α4β7. This low expression of other chemokine receptors was not a characteristic of all CXCR5$^+$ subsets, because the X5$^+$PD-1$^+$ subset showed strong expression of CXCR3, CCR5, and α4β7 (Fig. 1E). These results also revealed that the X5$^-$PD-1$^+$ CD4 subset was distinct from other GC Tfh cells and non-Tfh cell subsets because they showed strong expression of all other chemokine receptors studied.

Rapid enrichment of CXCR3$^+$ GC Tfh cells during chronic SIV infection

We next investigated the influence of SIV infection on the relative proportions of these five memory CD4 subsets and the expression of chemokine receptors CXCR3, CCR4, and CCR6 (Fig. 2). For this purpose, we used samples from a cohort of SIVmac251-infected RMs. The relative distribution of memory CD4 T cells was significantly altered in LNs of SIV-infected RMs compared with uninfected RMs (Fig. 2A). The frequency of X5$^+$PD-1$^+$ and GC Tfh CD4 T cells was higher and the frequency of the X5$^-$PD-1$^-$ subset was lower in the SIV-infected animals. However, the frequencies of X5$^-$PD-1$^+$ and X5$^+$PD-1$^-$ CD4$^+$ T cells were comparable. Interestingly, we observed a profound increase in CXCR3 expression on CXCR5$^+$ and CXCR5$^-$ memory CD4$^+$ T cells, and this increase was restricted primarily to the memory CD4 T cells that coexpressed PD-1, including GC Tfh cells (Fig. 2B). However, there was no significant difference in the expression of CCR4 on memory CD4 T cells (Fig. 2C). In contrast, the frequency of CCR6$^+$ memory CD4 T cells was dramatically lower on all memory CD4 T cell subsets, irrespective of their CXCR5 expression, demonstrating their preferential depletion during chronic SIV infection (Fig. 2D). We performed Boolean analysis to understand the coexpression of these chemokine receptors. The results revealed that, in SIV-naive animals, the majority of GC Tfh cells did not express CXCR3, CCR4, or CCR6 and that, during chronic SIV infection, the frequency of CXCR3$^+$ single-positive cells increased dramatically because the majority of these CXCR3$^+$ cells failed to coexpress CCR4 or CCR6 (Fig. 2E). These results demonstrated that chronic SIV infection significantly enhances the frequency of GC Tfh cells that coexpress high levels of Th1-associated chemokine receptor CXCR3.

CXCR3$^+$ GC Tfh cells are phenotypically and functionally distinct from CXCR3$^-$ GC Tfh cells

Previous studies showed that Th1 cells express CXCR3, and CXCR3 ligand–mediated interaction facilitates the migration of cells toward inflammatory sites, such as interfollicular and medullary zones of LNs (40). We next investigated whether CXCR3$^+$ GC Tfh cells are phenotypically or functionally distinct from CXCR3$^-$ GC Tfh cells. We compared the relative expression of Tfh cell markers (CXCR5, PD-1, ICOS) and Th1 cell markers (CCR7, T-box transcription factor T-bet) within the GC Tfh cell compartment (Fig. 3A). CXCR3$^+$ GC Tfh cells expressed significantly lower levels of CXCR5 and PD-1 compared with CXCR3$^-$ GC Tfh cells, although the difference was small; however, CXCR3$^+$ GC Tfh cells expressed higher levels of CCR7, ICOS, and T-bet (trend). The expression of Bcl-6 was comparable. These results suggested that CXCR3 expression identifies Th1-like GC Tfh cells in GCs.

To assess the functional cytokine profile, we sorted CXCR3$^+$ and CXCR3$^-$ GC Tfh cells and measured the production of IFN-γ, IL-21, and CD40L following stimulation with PMA/ionomycin. CXCR3$^+$, but not CXCR3$^-$, GC Tfh cells predominantly produced IFN-γ and IL-21, although the expression of CD40L was comparable between the two subsets (Fig. 3B). To assess the polyfunctional capacity of CXCR3$^+$ and CXCR3$^-$ GC Tfh cells in the LN during chronic SIV infection, we performed Boolean cytokine analysis. Interestingly, CXCR3$^+$ GC Tfh cell populations contained significantly higher proportions of triple producers (IFN-γ/IL-21/CD40L), double producers (IFN-γ/CD40L; IFN-γ/IL-21), and single producers (IFN-γ) (Fig. 3C). These data clearly suggest that CXCR3$^+$ GC Tfh cells are functionally different from CXCR3$^-$ GC Tfh cell populations.

To further understand the relationship between the subsets and viral replication, we studied the association between the frequency of CXCR3$^+$ and CXCR3$^-$ GC Tfh cells and plasma viremia and determined the levels of SIV DNA in these subsets. The frequency of CXCR3$^+$ and CXCR3$^-$ GC Tfh cells showed a direct correlation with plasma viremia (Fig. 3D), but a higher proportion of CXCR3$^+$ GC Tfh cells contained SIV DNA (Fig. 3E). Because CXCR3$^+$ GC Tfh cells contained higher levels of SIV DNA, we compared the relative expression of HIV coreceptor CCR5 and HIV binding protein α4β7 on CXCR3$^+$ and CXCR3$^-$ GC Tfh cells. Interestingly, CXCR3$^+$ GC Tfh cells expressed higher levels of CCR5 (p = 0.001), α4β7 (p = 0.008), and CCR5$^+$α4β7$^+$ double-positive cells (p = 0.04) compared with CXCR3$^-$ GC Tfh cells (Fig. 3F), suggesting the increased susceptibility of CXCR3$^+$ GC Tfh cells to HIV/SIV infection. Thus, our results clearly demonstrate that CXCR3$^+$ and CXCR3$^-$ GC Tfh cells are phenotypically and functionally different within GCs, suggesting the existence of two populations in the SIV-infected GC Tfh cell compartment. They also support the notion that CXCR3$^+$ GC Tfh cells could represent a Th1-biased Tfh cell subset (41, 42) in GCs during chronic SIV infection.

Chronic SIV infection results in the accumulation of IL-21$^+$ and IFN-γ$^+$ cells within the follicles

SIV infection induces follicular hyperplasia, which is associated with aberrant accumulation of Tfh cells producing IL-21 within GCs (43). Because we observed an enrichment of phenotypically and functionally different CXCR3$^+$ GC Tfh cells that produce IFN-γ during chronic SIV infection, we hypothesized that GCs of SIV-infected animals may also have higher levels of IFN-γ during chronic infection. Hence, we investigated the presence of cytokines IFN-γ and IL-21 within GCs in SIV-naive (n = 2) and

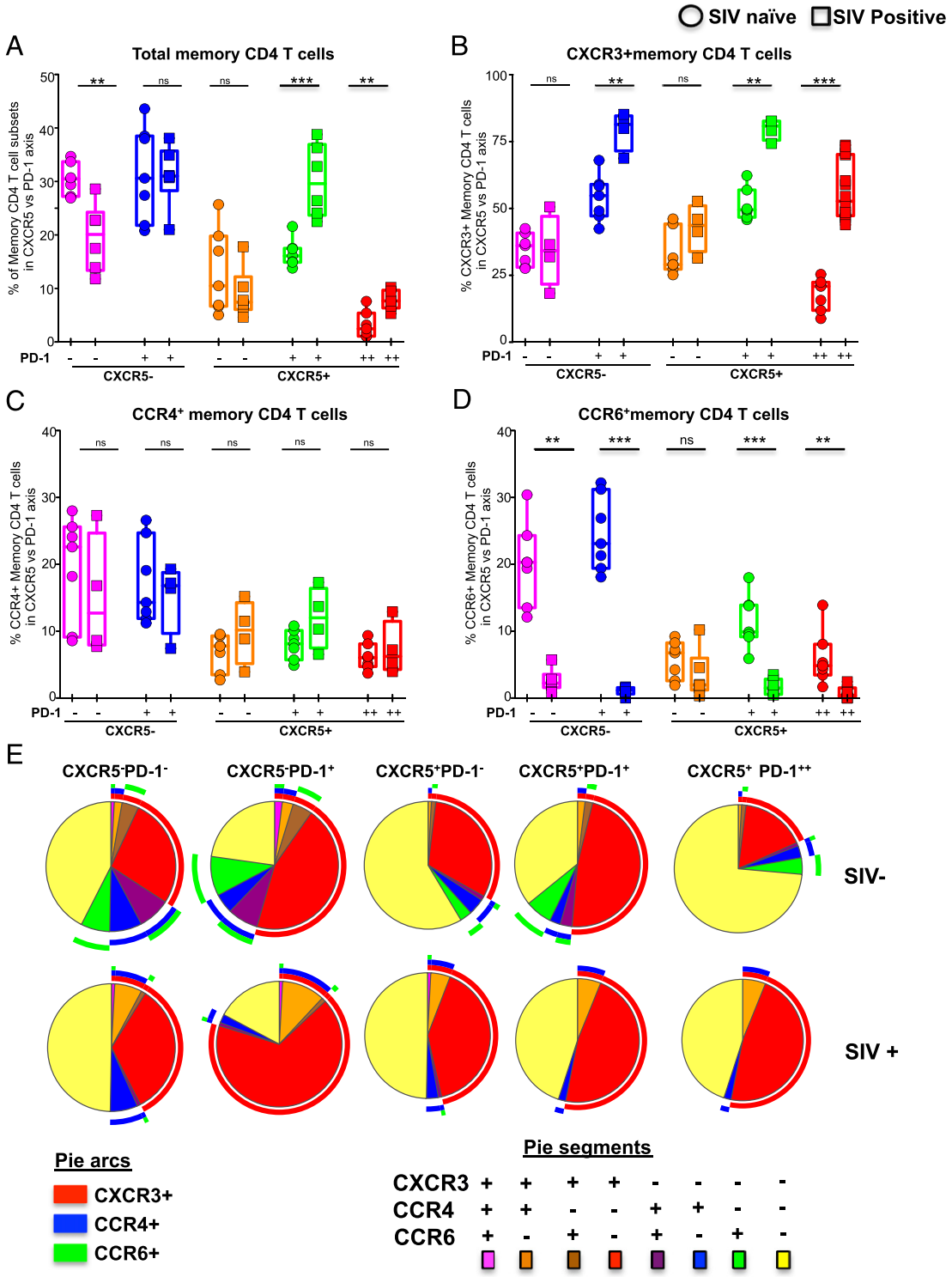

FIGURE 2. Enrichment of CXCR3$^+$ CD4 T cells in the LN during chronic SIV infection. (**A**) Relative distribution of five memory CD4 T cell subsets in the LN defined based on CXCR5 and PD-1 expression before and after (24 wk) SIV infection. Expression of CXCR3 (**B**), CCR4 (**C**) and CCR6 (**D**) on five memory CD4 T cell subsets defined based on CXCR5 and PD-1 expression before and 24 wk after SIV infection. (**E**) Pie charts summarizing the coexpression of chemokine receptors CXCR3, CCR4, and CCR6 on different memory CD4 T cell subsets. Red arcs identify CXCR3$^+$ populations, blue arcs identify CCR4$^+$ population, green arcs identify CCR6$^+$ population. Data for seven SIV$^-$ and SIV$^+$ animals are shown. $^{**}p < 0.01$, $^{***}p < 0.001$.

SIV-infected RMs with low ($n = 2$) and high ($n = 4$) plasma viral RNA levels using immunohistochemistry (Fig. 4). As shown before (35, 44), the number of hyperplastic follicles with GCs was significantly higher in chronically SIV-infected animals compared with SIV-naive animals (Fig. 4A, data not shown). Consistent with our previous findings (16, 43), the frequency of IL-21$^+$ cells in the follicles was significantly higher in SIV-infected animals with high viral load relative to SIV-naive animals (Fig. 4B). However, consistent with higher CXCR3 expression by flow cytometry, we also observed a significantly higher density of CD3$^+$IFN-γ^+ cells in the follicles of SIV-infected animals with high viral load relative to SIV-naive animals (Fig. 4C). In a limited number of RMs,

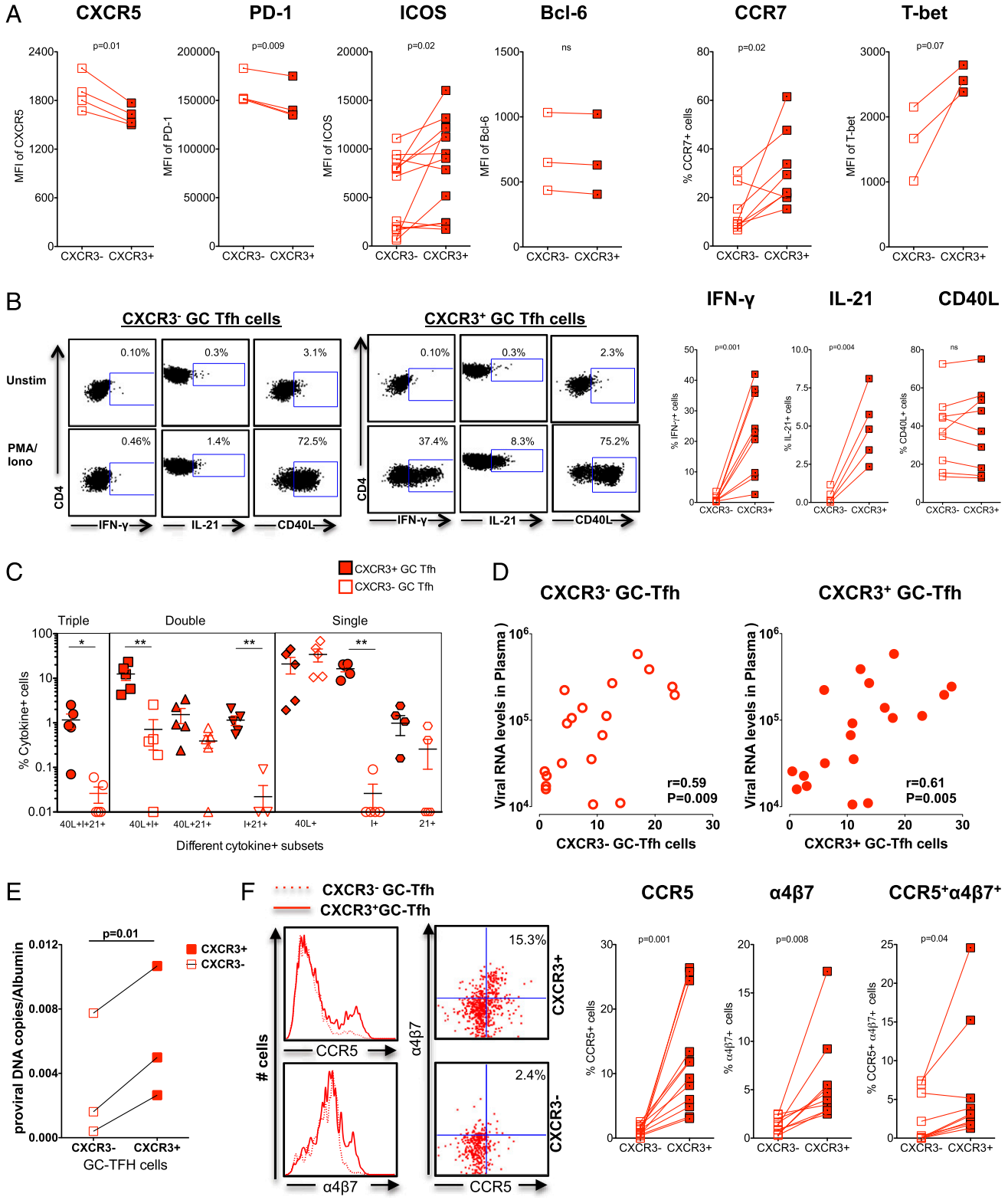

FIGURE 3. CXCR3$^+$ GC Tfh cells are phenotypically and functionally distinct from CXCR3$^-$ GC Tfh cells. (**A**) Expression of Tfh cell and Th1 cell markers on CXCR3$^+$ and CXCR3$^-$ GC Tfh cells (**B**) Expression of IFN-γ, IL-21 and CD40L by sorted CXCR3$^+$ and CXCR3$^-$ GC Tfh cells following stimulation with PMA/Ionomycin. Representative flow plots are shown on the left. (**C**) Boolean analysis determining coexpression of IFN-γ, IL-21 and CD40L. (**D**) Correlation between CXCR3$^+$ GC Tfh cells or CXCR3$^-$ GC Tfh cells and plasma viral RNA levels at 24 wk post-SIV infection. (**E**) Copies of SIV proviral DNA in sorted CXCR3$^+$ and CXCR3$^-$ GC Tfh cells. (**F**) Expression of CCR5 and α4β7 on CXCR3$^+$ and CXCR3$^-$ GC Tfh cells. $*p < 0.05$, $**p < 0.01$.

we confirmed that the IFN$^+$ cells are mostly CD4$^+$ (Supplemental Fig. 1A) and CD8$^-$ (Supplemental Fig. 1B). This increase in IL-21$^+$ or IFN-γ$^+$ cells was not observed in SIV-infected animals with lower viral load. Interestingly, the density of IL-21$^+$ and IFN-γ$^+$ cells in GCs correlated positively in animals with high viral load but not in animals with low viral load or in SIV-naive animals, demonstrating that IL-21$^+$ and IFN-γ$^+$ cells were expanded during chronic SIV infection (Fig. 4D). Collectively, these data demon-

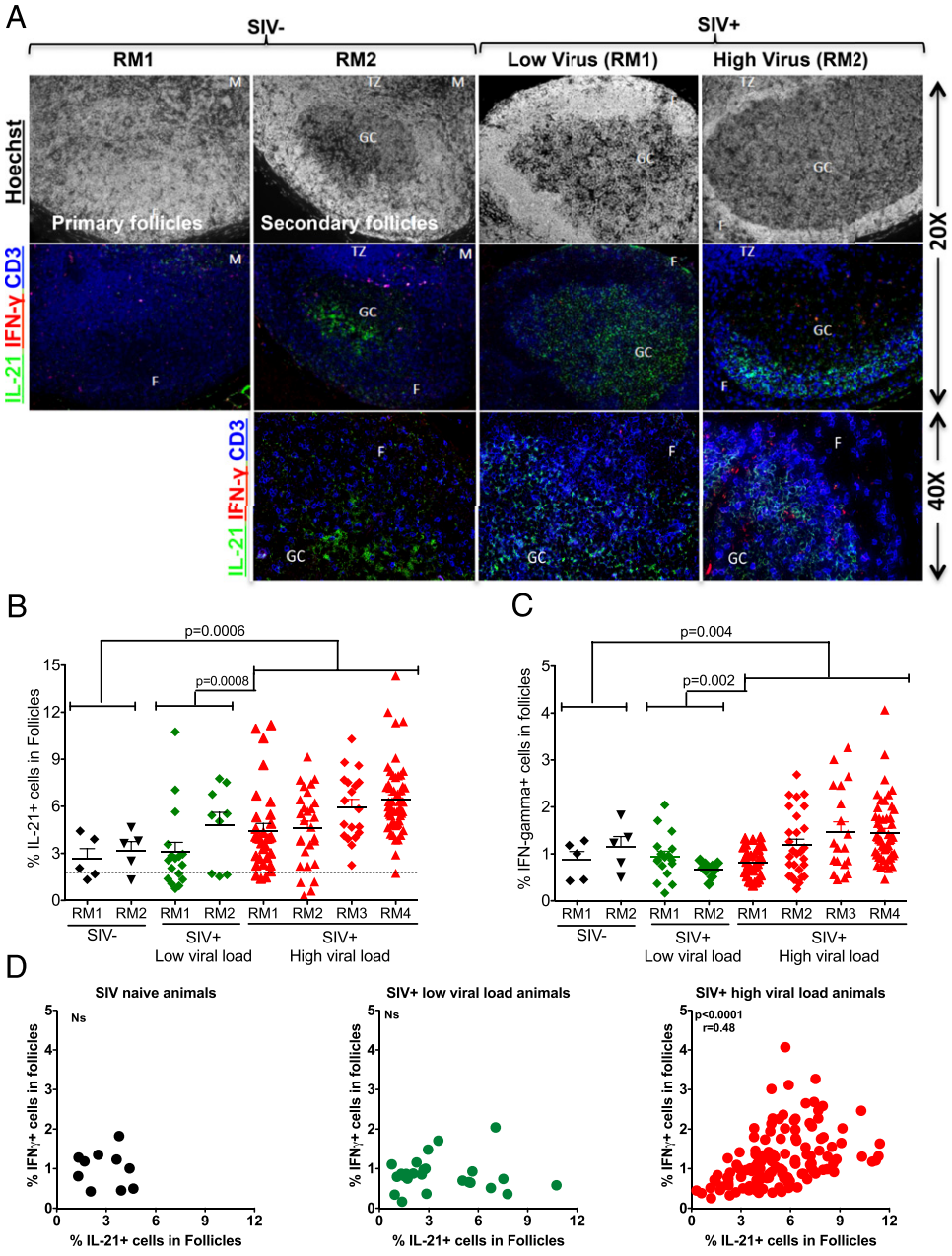

FIGURE 4. Chronic SIV infection results in accumulation of IL-21$^+$ and IFN-γ$^+$ cells within the follicles. (**A**) Representative IHC images showing IFN-γ$^+$ and IL-21$^+$ cells in the follicles, T cell zone, and medulla of LN of SIV-naive and SIV$^+$ RMs with low (<100 copies) and high (>10,000 copies) viral load. (**B**) Expression of IL-21 in follicles. (**C**) Expression of IFN-γ in follicles. Each dot indicates the percentage of cytokine intensity in one follicle. (**D**) Correlation between the expression of IFN-γ$^+$ and IL-21$^+$ cells in follicles.

strate that chronic uncontrolled SIV infection is associated with high levels of GC Tfh cells with Th1 phenotype, leading to enrichment of IFN-γ$^+$ cells within the follicles. These results provide important clues regarding GC-related hyperimmune responses in the context of disease progression during chronic SIV infection that may help to develop therapeutic strategies to limit lymphoid dysfunction during chronic SIV/HIV infection.

CXCR3$^+$ GC Tfh cells help B cells for Ab production during chronic SIV infection

Studies demonstrated that the differentiation of GC B cells into plasma cells is a Tfh cell–dependent process and that, in fact, a large proportion of Tfh cell functions are dedicated to B cell differentiation, survival, and proliferation. In addition, GC Tfh cells were shown to regulate Ab responses during HIV/SIV infection (12, 15, 16, 38, 45). To understand the nature of B cell help provided by CXCR3$^+$ and CXCR3$^-$ GC Tfh cells, we sorted CXCR3$^+$ and CXCR3$^-$ GC Tfh cells and CXCR5$^-$ cells, cocultured the various sorted subsets with autologous B cells in the presence and absence of staphylococcal enterotoxin B for 5–9 d, and measured B cell numbers and Ab production (15). We observed a significant increase in B cell numbers in the presence of CD4 T cells; interestingly, similar increases were observed in the presence of CXCR3$^+$ and CXCR3$^-$ GC Tfh cells (Fig. 5A), despite differences in their production of IFN-γ and IL-21 (Fig. 3). To test the effects of IFN-γ on IgG production by B cells, we sorted total B cells from three-SIV infected macaques and cultured them in the presence of IFN-γ (5 ng/ml) for 9 d and measured IgG levels in supernatants. Interestingly, addition of IFN-γ marginally increased the production of total IgG (Fig. 5B). However, in B cell coculture experiments, CXCR3$^+$ and CXCR3$^-$ GC Tfh cells induced production of IgG and IgG1 after 9 d of stimulation (Fig. 5C, 5D). Consistent with their potential to help B cells in vitro, we observed a strong direct association between the frequency of CXCR3$^+$ or CXCR3$^-$ GC Tfh cells and the concentration of SIV envelope-specific IgG (Fig. 5E) or IgG1 (Fig. 5F) in the serum. These results suggest that CXCR3$^+$ and CXCR3$^-$ GC Tfh cells contribute to the increased accumulation

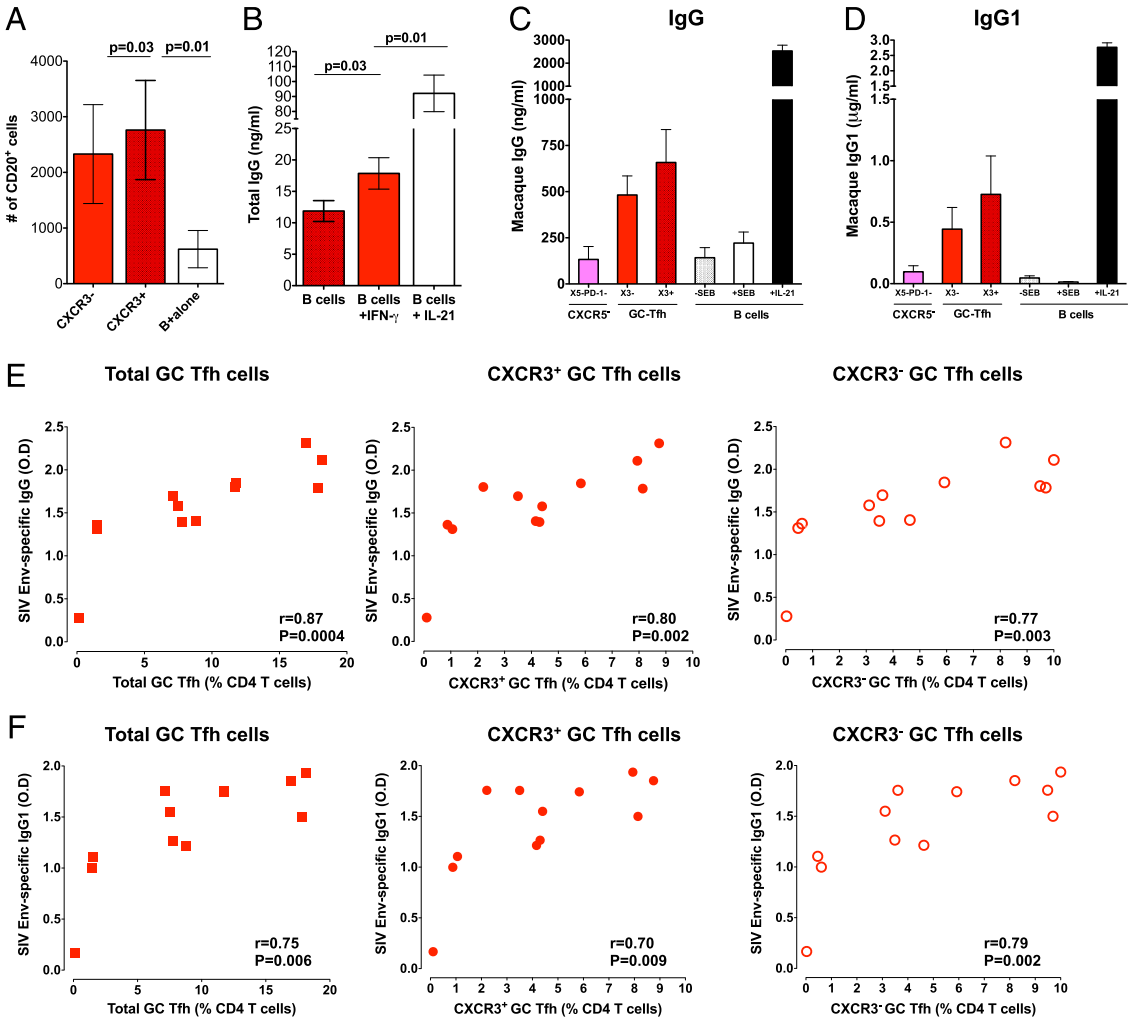

FIGURE 5. Both CXCR3$^+$ and CXCR3$^-$ GC Tfh cells help B cells equally irrespective of their functional difference. Sorted CXCR3$^+$ GC Tfh cells and CXCR3$^-$ GC Tfh cells from chronic SIV infected macaques were cocultured with autologous sorted B cells. (**A**) Total numbers of viable B cells at day 5 from the T and B coculture experiment. (**B**) IgG production by sorted B cells (B cell alone) from SIV infected RM in the presence of IFN-γ (5 ng/ml) or IL-21 (10 ng/ml). (**C**) IgG ($n = 4$) and (**D**) IgG1 ($n = 3$) concentrations at day 9 in T and B coculture experiments. (**E**) Correlation between SIV-envelop specific IgG (at 1:9000 dilution of sera) Ab levels and total, CXCR3$^+$ or CXCR3$^-$ GC Tfh cells at 24 wk post SIV infection. (**F**) Correlation between SIV-envelope–specific IgG1 (at 1:450 dilution of sera) Ab levels and total, CXCR3$^+$ or CXCR3$^-$ GC Tfh cells at 24 wk post-SIV infection.

of SIV-specific IgG and IgG1 during chronic SIV infection normally referred to as hypergammaglobulinemia (10).

Discussion

There is limited knowledge on the exact identity of various subsets of memory CD4$^+$ T cells that are present in the LN of SIV-naive and SIV-infected RMs. Recent studies identified the chemokine receptors CXCR3, CCR4, and CCR6 (46, 47) as surface markers for select lineages of CD4$^+$ T cells with distinct cytokine profiles and lineage-specific transcription factor expression (1) and established a link between CD4 T cell trafficking potential and immunologic function. Furthermore, recent progress in understanding the biology of human and mouse Tfh cells delineated functionally distinct subsets of memory Tfh cells in the circulation (31, 48, 49), suggesting that human blood memory Tfh cells coexpress chemokine receptors associated with other Th cell lineages, such as CXCR3 (Th1), CCR4 (Th2), and CCR6 (Th17) (28, 31). However, it remains to be established whether the analyses of blood memory Tfh cell subsets faithfully reflect GC Tfh cell responses in lymphoid organs of mice, macaques, and humans. In this study, we took advantage of the availability of LN samples from a well-characterized cohort of SIV-naive and SIV-infected RMs to delineate the different lineages of lymphoid memory CD4 T cell subsets and their function in RMs. Our results revealed that, in SIV-naive RMs, the majority of GC Tfh cells do not express chemokine receptors, such as CXCR3, CCR4, CCR6, and CCR7 and including the HIV coreceptor CCR5. This was in contrast to any other memory CD4 T cell subset in the LN, including other CXCR5$^+$ cells that expressed a diverse combination of these chemokine receptors. These results highlight an important finding that the majority of GC Tfh cells in SIV-naive RMs are not polarized to the Th1, Th2, or Th17 lineage.

Our results showed that chronic SIV infection modulates the phenotype of GC Tfh cells, such that they express high levels of Th1 lineage–associated chemokine receptor CXCR3, suggesting the emergence of Th1-biased Tfh cells. Consistent with this phenotype, CXCR3$^+$ Tfh cells, but not CXCR3$^-$ Tfh cells, produced the Th1 cytokine IFN-γ, and GCs of chronically SIV-infected noncontroller (viral load $>$ 10,000 copies) RMs had significantly higher levels of IFN-γ–producing CD4 T cells compared with SIV-naive and SIV-infected controller RMs (viral load $<$100 copies). The immune mechanisms that contributed to the induction of CXCR3$^+$ GC Tfh cells are not completely clear. A similar phenotype was observed for GC Tfh cells in mice infected

with lymphocytic choriomeningitis virus Clone 13 (23). In addition, this phenotype may not be specific to chronic infections because we recently observed this phenotype on GC Tfh cells after DNA/MVA vaccination of RMs in the presence of SIV envelope protein boost in alum (34). This raises the possibility that local inflammation alone can induce this phenotype on GC Tfh cells. Our results are also consistent with a recent study in macaques demonstrating that Th1 transcriptional factor T-bet is upregulated in Tfh cells isolated from the LN and spleen during chronic SIV infection (16, 18, 35, 36). In addition to GC Tfh cells, we observed an increase in CXCR3 expression on all other memory CD4 T cells in the LN, indicating that this effect is not restricted to GC Tfh cells.

Studies in humans delineated the susceptibility to HIV infection in different lineages of CD4 T cells during chronic HIV infection using CCR5 expression and compared with their level of integrated HIV DNA (44). In SIV-naive animals, Tfh cells, particularly GC Tfh cells, expressed very low levels of CCR5 (16, 39), yet they were found to harbor high levels of SIV DNA during chronic infection, raising some interesting questions about their infection kinetics/mechanism. However, when analyzed based on the expression of Th1 marker CXCR3, we found that $CXCR3^+$ GC Tfh cells express higher levels of CCR5 and $\alpha4\beta7$, as well as harbor higher copies of SIV DNA, indicating an increased susceptibility of these cells to SIV infection. Moreover, the data presented in this article demonstrate a marked expansion of these $CXCR3^+$ GC Tfh cells during SIV infection. Similar findings were reported in the blood of HIV-infected individuals, as well as in a mouse model of HIV infection, where $CXCR3^+$ CD4 T cells preferentially expressed the HIV coreceptor CCR5 (44, 50). Hence, we speculate that $CXCR3^+CCR5^+\alpha4\beta7^+$ GC Tfh cell subsets may have the capacity to maintain a dynamic viral reservoir in GCs under antiretroviral therapy. Thus, we established a link between Th1 and Tfh cell subsets during SIV infection, demonstrating their distribution, phenotype, and function, as well as the potential dynamics of SIV infection in this compartment. These findings may open novel therapeutic approaches for targeting the viral reservoirs in $CXCR3^+$ and $CXCR3^-$ GC Tfh cell subsets.

In an attempt to understand the contribution of $CXCR3^+$ GC Tfh cells to antiviral humoral immunity, we determined the B cell helper potential of these cells and compared it with that of $CXCR3^-$ GC Tfh cells; we found that $CXCR3^+$ and $CXCR3^-$ GC Tfh cells possess B cell helper potential. Consistent with this in vitro finding, $CXCR3^+$ and $CXCR3^-$ GC Tfh cells had the capacity to help B cell proliferation equally when cocultured with autologous B cells and showed a direct association with SIV-specific serum IgG and IgG1 during chronic SIV infection. This is consistent with the ability of these cells to express molecules associated with B cell help, such as ICOS and CD40L. This contrasts with what was reported for circulating $CXCR5^+$ CD4 T cells in human blood; $CXCR3^-CXCR5^+$ cells, not $CXCR3^+$ $CXCR5^+$ cells, were shown to help B cells in vitro (48). However, another human study demonstrated that circulating $CXCR3^+$ $CXCR5^+ICOS^+$ cells induced following seasonal influenza vaccination help memory B cells and correlate with the development of flu-specific Ab responses (28, 51). It is important to note that, in all of these studies, the B cell helper potential seems to correlate with the ability of $CXCR5^+$ cells to express ICOS and CD40L, and there may be differences in the expression of these molecules on $CXCR3^+$ and $CXCR3^-$ cells between humans and macaques, as well as between blood and LN.

We think that a potential influence of $CXCR3^+$ Tfh cells on HIV/SIV pathogenesis during chronic infection could be their ability to induce autoantibodies, a profound feature of chronic HIV/SIV infections. A recent study showed that excessive IFN-γ signaling in GCs due to excessive production of IFN-γ by T cells leads to accumulation of GC Tfh cells and sustained GC reaction and formation of autoantibodies (42). Further, studies also showed that IFN-γ contributes to the induction of B lymphocyte stimulating factor (BAFF), and Th1-polarized CD4 T cells contribute to production of autoantibodies, even in the absence CD40-CD40L signaling (42, 52), which was shown to be deficient during chronic HIV (53) and SIV (54, 55) infections.

In the current study, $CXCR3^+$ and $CXCR3^-$ GC Tfh cells are associated with the increased amount of SIV-envelope–specific Abs during chronic SIV infection. However, a recent study in HIV-infected individuals described a subset of circulating memory Tfh cells that is negative for CXCR3 ($CXCR3^-CXCR5^+CD4^+$), helps B cells, and is present in high numbers in HIV-infected individuals who generate broadly neutralizing Abs (29). Taking this into account, we further speculate that $CXCR3^+$ and $CXCR3^-$ GC Tfh cells help B cells; however, $CXCR3^+$ GC Tfh cells may also contribute to the induction of autoantibodies through production of IFN-γ, as discussed above. In addition, higher CCR5 and $\alpha4\beta7$ expression by $CXCR3^+$ GC Tfh cells may contribute to sustained replication of virus during chronic infection and higher viral reservoirs during antiretroviral therapy. A better understanding of the early differentiation process and the developmental relationship between these cells in the LN during HIV/SIV infection is critical for the establishment of reliable CD4 T cell correlates for monitoring infection or vaccine-associated Ab responses during HIV/SIV infection.

Acknowledgments

We thank Dr. Joshy Jacob for the suggestion to perform B cell coculture assays using sorted cells. We thank the animal care and veterinary staff of YNPRC, Benton Lawson and Melon Tekola Nega for virology assays, and Dr. Kiran Gill and Dr. Barbara Cervasi for help with flow cytometry and flow sorting. We also thank the NIH AIDS Research and Reference Reagent Program for the provision of peptides.

Disclosures

The authors have no financial conflicts of interest.

References

1. O'Shea, J. J., and W. E. Paul. 2010. Mechanisms underlying lineage commitment and plasticity of helper CD4+ T cells. *Science* 327: 1098–1102.
2. Pepper, M., and M. K. Jenkins. 2011. Origins of CD4(+) effector and central memory T cells. *Nat. Immunol.* 12: 467–471.
3. Bluestone, J. A., C. R. Mackay, J. J. O'Shea, and B. Stockinger. 2009. The functional plasticity of T cell subsets. *Nat. Rev. Immunol.* 9: 811–816.
4. Sallusto, F., J. Geginat, and A. Lanzavecchia. 2004. Central memory and effector memory T cell subsets: function, generation, and maintenance. *Annu. Rev. Immunol.* 22: 745–763.
5. Kim, C. H., L. S. Rott, I. Clark-Lewis, D. J. Campbell, L. Wu, and E. C. Butcher. 2001. Subspecialization of CXCR5+ T cells: B helper activity is focused in a germinal center-localized subset of CXCR5+ T cells. *J. Exp. Med.* 193: 1373–1381.
6. Breitfeld, D., L. Ohl, E. Kremmer, J. Ellwart, F. Sallusto, M. Lipp, and R. Förster. 2000. Follicular B helper T cells express CXC chemokine receptor 5, localize to B cell follicles, and support immunoglobulin production. *J. Exp. Med.* 192: 1545–1552.
7. Moser, B., P. Schaerli, and P. Loetscher. 2002. CXCR5(+) T cells: follicular homing takes center stage in T-helper-cell responses. *Trends Immunol.* 23: 250–254.
8. Fazilleau, N., L. J. McHeyzer-Williams, H. Rosen, and M. G. McHeyzer-Williams. 2009. The function of follicular helper T cells is regulated by the strength of T cell antigen receptor binding. *Nat. Immunol.* 10: 375–384.
9. Crotty, S. 2011. Follicular helper CD4 T cells (TFH). *Annu. Rev. Immunol.* 29: 621–663.
10. Lindqvist, M., J. van Lunzen, D. Z. Soghoian, B. D. Kuhl, S. Ranasinghe, G. Kranias, M. D. Flanders, S. Cutler, N. Yudanin, M. I. Muller, et al. 2012. Expansion of HIV-specific T follicular helper cells in chronic HIV infection. *J. Clin. Invest.* 122: 3271–3280.

11. Perreau, M., A. L. Savoye, E. De Crignis, J. M. Corpataux, R. Cubas, E. K. Haddad, L. De Leval, C. Graziosi, and G. Pantaleo. 2013. Follicular helper T cells serve as the major CD4 T cell compartment for HIV-1 infection, replication, and production. *J. Exp. Med.* 210: 143–156.
12. Cubas, R. A., J. C. Mudd, A. L. Savoye, M. Perreau, J. van Grevenynghe, T. Metcalf, E. Connick, A. Meditz, G. J. Freeman, G. Abesada-Terk, Jr., et al. 2013. Inadequate T follicular cell help impairs B cell immunity during HIV infection. *Nat. Med.* 19: 494–499.
13. Pallikkuth, S., M. Sharkey, D. Z. Babic, S. Gupta, G. W. Stone, M. A. Fischl, M. Stevenson, and S. Pahwa. 2015. Peripheral T follicular helper cells are the major HIV reservoir within central memory CD4 T cells in peripheral blood from chronically HIV-infected individuals on combination antiretroviral therapy. J. Virol. 90: 2718–2728.
14. Hong, J. J., P. K. Amancha, K. Rogers, A. A. Ansari, and F. Villinger. 2012. Spatial alterations between CD4(+) T follicular helper, B, and CD8(+) T cells during simian immunodeficiency virus infection: T/B cell homeostasis, activation, and potential mechanism for viral escape. *J. Immunol.* 188: 3247–3256.
15. Petrovas, C., T. Yamamoto, M. Y. Gerner, K. L. Boswell, K. Wloka, E. C. Smith, D. R. Ambrozak, N. G. Sandler, K. J. Timmer, X. Sun, et al. 2012. CD4 T follicular helper cell dynamics during SIV infection. *J. Clin. Invest.* 122: 3281–3294.
16. Mylvaganam, G. H., V. Velu, J. J. Hong, S. Sadagopal, S. Kwa, R. Basu, B. Lawson, F. Villinger, and R. R. Amara. 2014. Diminished viral control during simian immunodeficiency virus infection is associated with aberrant PD-1hi CD4 T cell enrichment in the lymphoid follicles of the rectal mucosa. *J. Immunol.* 193: 4527–4536.
17. Chowdhury, A., P. M. Del Rio Estrada, G. K. Tharp, R. P. Trible, R. R. Amara, A. Chahroudi, G. Reyes-Teran, S. E. Bosinger, and G. Silvestri. 2015. Decreased T follicular regulatory cell/T follicular helper cell (TFH) in simian immunodeficiency virus-infected rhesus macaques may contribute to accumulation of TFH in chronic infection. [Published erratum appears in 2015 *J. Immunol.* 195: 5843]. J. Immunol. 195: 3237–3247.
18. Xu, H., X. Wang, N. Malam, P. P. Aye, X. Alvarez, A. A. Lackner, and R. S. Veazey. 2015. Persistent simian immunodeficiency virus infection drives differentiation, aberrant accumulation, and latent infection of germinal center follicular T helper cells. *J. Virol.* 90: 1578–1587.
19. Petrovas, C., and R. A. Koup. 2014. T follicular helper cells and HIV/SIV-specific antibody responses. *Curr. Opin. HIV AIDS* 9: 235–241.
20. Onabajo, O. O., J. George, M. G. Lewis, and J. J. Mattapallil. 2013. Rhesus macaque lymph node PD-1(hi)CD4+ T cells express high levels of CXCR5 and IL-21 and display a CCR7(lo)ICOS+Bcl6+ T-follicular helper (Tfh) cell phenotype. *PLoS One* 8: e59758.
21. Xu, Y., C. Weatherall, M. Bailey, S. Alcantara, R. De Rose, J. Estaquier, K. Wilson, K. Suzuki, J. Corbeil, D. A. Cooper, et al. 2013. Simian immunodeficiency virus infects follicular helper CD4 T cells in lymphoid tissues during pathogenic infection of pigtail macaques. *J. Virol.* 87: 3760–3773.
22. Pissani, F., and H. Streeck. 2014. Emerging concepts on T follicular helper cell dynamics in HIV infection. *Trends Immunol.* 35: 278–286.
23. Fahey, L. M., E. B. Wilson, H. Elsaesser, C. D. Fistonich, D. B. McGavern, and D. G. Brooks. 2011. Viral persistence redirects CD4 T cell differentiation toward T follicular helper cells. *J. Exp. Med.* 208: 987–999.
24. Glatman Zaretsky, A., J. J. Taylor, I. L. King, F. A. Marshall, M. Mohrs, and E. J. Pearce. 2009. T follicular helper cells differentiate from Th2 cells in response to helminth antigens. *J. Exp. Med.* 206: 991–999.
25. Crotty, S. 2014. T follicular helper cell differentiation, function, and roles in disease. *Immunity* 41: 529–542.
26. Milpied, P. J., and M. G. McHeyzer-Williams. 2013. High-affinity IgA needs TH17 cell functional plasticity. *Nat. Immunol.* 14: 313–315.
27. Schmitt, N., S. E. Bentebibel, and H. Ueno. 2014. Phenotype and functions of memory Tfh cells in human blood. *Trends Immunol.* 35: 436–442.
28. Bentebibel, S. E., S. Lopez, G. Obermoser, N. Schmitt, C. Mueller, C. Harrod, E. Flano, A. Mejias, R. A. Albrecht, D. Blankenship, et al. 2013. Induction of ICOS+CXCR3+CXCR5+ TH cells correlates with antibody responses to influenza vaccination. *Sci. Transl. Med.* 5: 176ra32.
29. Locci, M., C. Havenar-Daughton, E. Landais, J. Wu, M. A. Kroenke, C. L. Arlehamn, L. F. Su, R. Cubas, M. M. Davis, A. Sette, et al; International AIDS Vaccine Initiative Protocol C Principal Investigators. 2013. Human circulating PD-1+CXCR3-CXCR5+ memory Tfh cells are highly functional and correlate with broadly neutralizing HIV antibody responses. *Immunity* 39: 758–769.
30. Rivino, L., M. Messi, D. Jarrossay, A. Lanzavecchia, F. Sallusto, and J. Geginat. 2004. Chemokine receptor expression identifies Pre-T helper (Th)1, Pre-Th2, and nonpolarized cells among human CD4+ central memory T cells. *J. Exp. Med.* 200: 725–735.
31. Boswell, K. L., R. Paris, E. Boritz, D. Ambrozak, T. Yamamoto, S. Darko, K. Wloka, A. Wheatley, S. Narpala, A. McDermott, et al. 2014. Loss of circulating CD4 T cells with B cell helper function during chronic HIV infection. *PLoS Pathog.* 10: e1003853.
32. Kwa, S., S. Sadagopal, X. Shen, J. J. Hong, S. Gangadhara, R. Basu, B. Victor, S. S. Iyer, C. C. LaBranche, D. C. Montefiori, et al. 2015. CD40L-adjuvanted DNA/MVA simian immunodeficiency virus (SIV) vaccine enhances protection against neutralization resistant mucosal SIV infection. *J. Virol.* 89: 4690–4695.
33. Velu, V., K. Titanji, B. Zhu, S. Husain, A. Pladevega, L. Lai, T. H. Vanderford, L. Chennareddi, G. Silvestri, G. J. Freeman, et al. 2009. Enhancing SIV-specific immunity in vivo by PD-1 blockade. *Nature* 458: 206–210.
34. Iyer, S. S., S. Gangadhara, B. Victor, R. Gomez, R. Basu, J. J. Hong, C. Labranche, D. C. Montefiori, F. Villinger, B. Moss, and R. R. Amara. 2015. Codelivery of envelope protein in alum with MVA vaccine induces CXCR3-biased CXCR5+ and CXCR5- CD4 T cell responses in rhesus macaques. *J. Immunol.* 195: 994–1005.
35. Moukambi, F., H. Rabezanahary, V. Rodrigues, G. Racine, L. Robitaille, B. Krust, G. Andreani, C. Soundaramourty, R. Silvestre, M. Laforge, and J. Estaquier. 2015. Early loss of splenic Tfh cells in SIV-infected rhesus macaques. [Published erratum appears in 2016 PLoS Pathog. 12: e1005393.] *PLoS Pathog.* 11: e1005287.
36. Miles, B., S. M. Miller, J. M. Folkvord, A. Kimball, M. Chamanian, A. L. Meditz, T. Arends, M. D. McCarter, D. N. Levy, E. G. Rakasz, et al. 2015. Follicular regulatory T cells impair follicular T helper cells in HIV and SIV infection. *Nat. Commun.* 6: 8608.
37. Xu, H., X. Wang, A. A. Lackner, and R. S. Veazey. 2014. PD-1(HIGH) follicular CD4 T helper cell subsets residing in lymph node germinal centers correlate with B cell maturation and IgG production in rhesus macaques. *Front. Immunol.* 5: 85.
38. Acosta-Rodriguez, E. V., L. Rivino, J. Geginat, D. Jarrossay, M. Gattorno, A. Lanzavecchia, F. Sallusto, and G. Napolitani. 2007. Surface phenotype and antigenic specificity of human interleukin 17-producing T helper memory cells. *Nat. Immunol.* 8: 639–646.
39. Fukazawa, Y., H. Park, M. J. Cameron, F. Lefebvre, R. Lum, N. Coombes, E. Mahyari, S. I. Hagen, J. Y. Bae, M. D. Reyes, III, et al. 2012. Lymph node T cell responses predict the efficacy of live attenuated SIV vaccines. *Nat. Med.* 18: 1673–1681.
40. Groom, J. R., J. Richmond, T. T. Murooka, E. W. Sorensen, J. H. Sung, K. Bankert, U. H. von Andrian, J. J. Moon, T. R. Mempel, and A. D. Luster. 2012. CXCR3 chemokine receptor-ligand interactions in the lymph node optimize CD4+ T helper 1 cell differentiation. *Immunity* 37: 1091–1103.
41. Pepper, M., A. J. Pagán, B. Z. Igyártó, J. J. Taylor, and M. K. Jenkins. 2011. Opposing signals from the Bcl6 transcription factor and the interleukin-2 receptor generate T helper 1 central and effector memory cells. *Immunity* 35: 583–595.
42. Lee, S. K., D. G. Silva, J. L. Martin, A. Pratama, X. Hu, P. P. Chang, G. Walters, and C. G. Vinuesa. 2012. Interferon-γ excess leads to pathogenic accumulation of follicular helper T cells and germinal centers. *Immunity* 37: 880–892.
43. Hong, J. J., P. K. Amancha, K. A. Rogers, C. L. Courtney, C. Havenar-Daughton, S. Crotty, A. A. Ansari, and F. Villinger. 2014. Early lymphoid responses and germinal center formation correlate with lower viral load set points and better prognosis of simian immunodeficiency virus infection. *J. Immunol.* 193: 797–806.
44. Gosselin, A., P. Monteiro, N. Chomont, F. Diaz-Griffero, E. A. Said, S. Fonseca, V. Wacleche, M. El-Far, M. R. Boulassel, J. P. Routy, et al. 2010. Peripheral blood CCR4+CCR6+ and CXCR3+CCR6+CD4+ T cells are highly permissive to HIV-1 infection. *J. Immunol.* 184: 1604–1616.
45. Blackburn, M. J., M. Zhong-Min, F. Caccuri, K. McKinnon, L. Schifanella, Y. Guan, G. Gorini, D. Venzon, C. Fenizia, N. Binello, et al. 2015. Regulatory and Helper Follicular T Cells and antibody avidity to simian immunodeficiency virus glycoprotein 120. *J. Immunol.* 195: 3227–3236.
46. Annunziato, F., L. Cosmi, F. Liotta, E. Maggi, and S. Romagnani. 2014. Human Th1 dichotomy: origin, phenotype and biologic activities. *Immunology.*
47. Sallusto, F., D. Lenig, C. R. Mackay, and A. Lanzavecchia. 1998. Flexible programs of chemokine receptor expression on human polarized T helper 1 and 2 lymphocytes. *J. Exp. Med.* 187: 875–883.
48. Morita, R., N. Schmitt, S. E. Bentebibel, R. Ranganathan, L. Bourdery, G. Zurawski, E. Foucat, M. Dullaers, S. Oh, N. Sabzghabaei, et al. 2011. Human blood CXCR5(+)CD4(+) T cells are counterparts of T follicular cells and contain specific subsets that differentially support antibody secretion. *Immunity* 34: 108–121.
49. Hale, J. S., B. Youngblood, D. R. Latner, A. U. Mohammed, L. Ye, R. S. Akondy, T. Wu, S. S. Iyer, and R. Ahmed. 2013. Distinct memory CD4+ T cells with commitment to T follicular helper- and T helper 1-cell lineages are generated after acute viral infection. *Immunity* 38: 805–817.
50. Allam, A., S. Majji, K. Peachman, L. Jagodzinski, J. Kim, S. Ratto-Kim, W. Wijayalath, M. Merbah, J. H. Kim, N. L. Michael, et al. 2015. TFH cells accumulate in mucosal tissues of humanized-DRAG mice and are highly permissive to HIV-1. *Sci. Rep.* 5: 10443.
51. Pallikkuth, S., A. Parmigiani, S. Y. Silva, V. K. George, M. Fischl, R. Pahwa, and S. Pahwa. 2012. Impaired peripheral blood T-follicular helper cell function in HIV-infected nonresponders to the 2009 H1N1/09 vaccine. *Blood* 120: 985–993.
52. Gorbacheva, V., R. Fan, X. Wang, W. M. Baldwin, III, R. L. Fairchild, and A. Valujskikh. 2015. IFN-γ production by memory helper T cells is required for CD40-independent alloantibody responses. *J. Immunol.* 194: 1347–1356.
53. Zhang, R., C. J. Fichtenbaum, D. A. Hildeman, J. D. Lifson, and C. Chougnet. 2004. CD40 ligand dysregulation in HIV infection: HIV glycoprotein 120 inhibits signaling cascades upstream of CD40 ligand transcription. *J. Immunol.* 172: 2678–2686.
54. Klatt, N. R., C. L. Vinton, R. M. Lynch, L. A. Canary, J. Ho, P. A. Darrah, J. D. Estes, R. A. Seder, S. L. Moir, and J. M. Brenchley. 2011. SIV infection of rhesus macaques results in dysfunctional T- and B-cell responses to neo and recall *Leishmania major* vaccination. *Blood* 118: 5803–5812.
55. Brice, G. T., A. E. Mayne, K. Leighton, F. Villinger, J. S. Allan, and A. A. Ansari. 1999. Studies of CD40L expression by lymphoid cells from experimentally and naturally SIV-infected nonhuman primate species. *J. Med. Primatol.* 28: 49–56.